Contents

5. Pioneer Venus Spacecraft Charging Model

P.A. Robinson, Jr. and A.B. Holman
Hughes Aircraft Company
Space and Communications Group
El Segundo, California

Abstract

Large potential differences between parts of the spacecrafts or between the spacecraft and the plasma will cause instruments ti, give misleading or meahingless data. Potentials and currents at various locations on the Pioneer Venus Orbiter are predicted by constructing ah electrical mbdel of the spacecraft and the environment, and Calculating the response of the electrical model to the environment model.

Five environment models were constructed to represent the solar wind and the upper, middle, and lower ionosphere of Venus. The spacecraft structure was modeled With over 140 passive electrical elemehts representing structural elements of the spacecraft. Electroh, ion, secondary electron, and photocurrents to the spacecraft from the plasma were calculated, ignoring sheath effects.

Ih all but one case, potentials of interest were less than 1 volt. Potential differences between widely separated points on the equipment shelf were less than 1 mV. The one area of concern is the solar panel potential when the orbiter is passing through the bowshock region. Here we assumed a high photocurrent and a low density, low temperature plasma, wtth solar panel potentials approaching 5 volts positive. Some experimenters indtcated thts would present a problem in ihterpreting results. Further study is needed to clarify thls issue; otherwise, spacecraft potentials are well within design levels.

Work performed by Hughes for Ames Research Center under Contract NAS 28300.

1. INTRODUCTION

Spacecraft for two Pioneer Vanun missions nrc beíng build by Hughes Aircraft Company for NASA Ames Research Center. In tho multiprobe mission, a large entry probe will make detailed measurements of the Venusian atmosphere and clouds. Three small probes will simultaneously sample conditions at widely separated points, The probe bus will make upper atmospheric measurements prior to its entry and burnup. In the orbiter mission, a spacecraft will circle the planet for a Venusian year (225 days), examining long term and glpbal effects. The orblter wtll be placed in a highly inclined elliptical orbit with a low altitude, midlatitude periapsis location. Most of the measurements will be taken during the periapsis pass.

Figure 1 shows the Pioneer Venus Orbiter. There is a condueting mesh over the forward end of the spacecraft to ensure a uniform charge distribution. Table 1 lists the instruments on th&orbiter that are concetned with the charge state of the spacecraft. None of the experimenters felt their instrument would influence the charge state of the spacecraft.

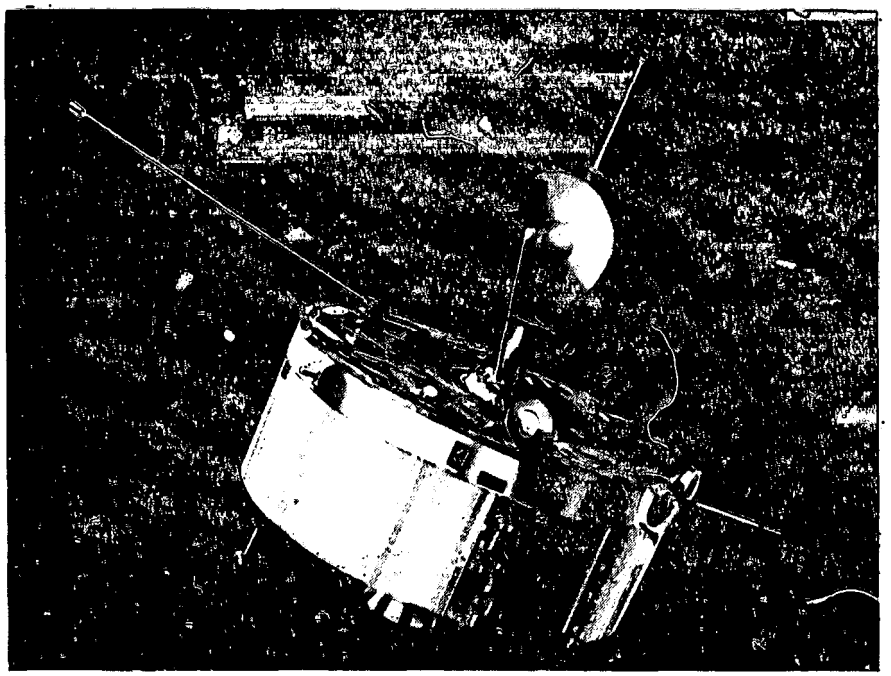

Figure 1. Pioneer Venus Orbiter

Table 1. Experiments Concerned with Charge State of Spacecraft

Instrument	Operating Altitude	Important Features
Ion mass spectrometer Dr. Harry Taylor	<5000 km	No external potentials; current $\geq 5 \times 16^{14}$ A. 2 in. dia aperture; would prefer negatively charged spacecraft
Electron temperature probe Dr. Larry Brace	≥6000 km	Exposed potentials vary from -5 to +7 V; total area ~13 cm^2; single probe area = 4 cm2
Retarding potential analyzer Dr. William Knudsen	All	Exposed potential +6 V current to instrument could be as high as 10^{-4} A; aperture diameter = 8 tm; would prefer space. craft potential from -1 to -5 V.
Plasma analyzer Dr. John Wolfe	All	Potential ±700 V; maximum current 10^{-12} A; aperture area = 1 cm^2
Electric field detector Dr. Fred Scarf	All	No exposed potentials; measures potential difference across instrument at frequencies above 100 Hz

2. CHARGED PARTICLE ENVIRONMENT

The charged particle environment for the Pioneer Venus Orbiter mission is an upper bound on empirical information obtained from various sources.[1-4] The model covers the full range of altitudes where scientific packages on the orbiter vehicle are operational. The model is summarized in Table 2.

Table 2. Pioneer Venus Orbiter - Charged Particle Environment

Region Label	Environment Component	Altitude Range, km	Charged Particles	Maximum Densities, per cm^3	Energy Levels, eV
I	Solar wind	∞ to 1000	Protons electrons	10 10	10 to 100 10 to 100
II	Upper ionosphere	1000 to 700	Ions (CO_2+) electrons	10^2 10^2	<0.1 <0.1
III	Middle ionosphere	700 to 350	Ions (CO_2+) electrons	10^3 10^3	<0.1 <0.1
IV	Lower ionosphere 1	350 to 200	Ions (CO_2+) electrons	5×10^4 5×10^4	<0.1 <0.1
V	Lower ionosphere 2	200 to 150	Ions (CO_2+) electrons	5×10^5 5×10^5	~0.06 ~0.06

A cosmic ray background[5] will be present at all altitudes. Since the current densities are low and the particle energies high, there will be negligible contribution to a surface charge or potential buildup bn the orbiter exterior surfaces from this source. The solar wind component of the environment dominates down to an altitude of approximately 1000 km, the bowshock region (actual altitude strongly dependeht on vehicle trajectory). The ionosphere begins tb develop at lower altitudes and particle and current densities peak at an altitude in the range of 150 to 200 km (~ 500°K thermosphere).

The ionosphere is extremely dynamic and the altitudes bounding the regions of interest should not be taken as rigid divisions. In addition, the solar radiation (~ 5750°K blackbody, 2.7×10^{-4} ergs/cm^2 sec) at Venus contributes strongly to the spacecraft charge for the orbiter because of the effect of photoemission from the spacecraft external surfaces.

Electron and idn currents, photoemission currents, alid secondary electron currents are included as appropriate. Tables 3 and 4 list current density (amperes per square centimeter) used in calculations for each region. These current densities are one-half the expected maximum thermal currents. The secondary electron current is dependent on a parameter E_{max}, the energy at maximum secbndary electron emission. Table 4 lists the Becondary electron emission for two typical E_{max} and $S_{max} = 1$. S_{max} is the number of secondary electrons emitted at E_{max}. The resistivity of the plaama is calculated from kinetic theory,[6] In calculating the resistance to the plasma from each element, the Debye length[6] was used as the length through the plasma. Table 5 lists the terms included in a power series expansion of current versus potential.

KEY FOR TABLES 3 THROUGH 5

ALT = altitude range

N_e = electron density, electron/cm3

kT_e = electron temperature, eV

$\lambda_D = \left(\frac{kT}{4\pi N_e e^2}\right)^{1/2}$ = Debye length, cm

$\eta = \frac{m_e c^2 \nu}{N_e e^2}$ = kinetic theory resistivity;

ν = collision frequency

J_e = electron current density

J_i = ion current density

$J_{e/e}$ = secondary electron curfent density

J_{hu} = photoemission current density

J = total current density

Table 3. Plasma Parameters

Region	Altitude, km	N_e, cm^{-3}	kT_e, eV	λ_D, cm	η, ohm-cm
I Solar wind	∞ to 1000	10	100	2.35×10^{3}	3.194×10^{3}
II	1000 tb 700	100	6.1	23.5	2.8×10^{8}
III	700 to 356	10^{3}	0.1	7.43	2.5×10^{7}
IV	350 to 200	10^{4}	0.1	1.05	5.0×10^{6}
V	200 to 150	5.0×10^{5}	0.66	0.26	5.0×10^{4}

Table 4. Plasma Currents Used in Calculations*

Region	J_{e_o}, A/cm^2	J_{i_o}, A/cm^2	$J_{e/_{eo}}$, E = 300 A/cm^2	$J_{e/_{eo}}$, E-400	J_{hu}, A/cm^2
I Solar wind	1.34×10^{-10}	3.13×10^{-12}	1.38×10^{-12}	1.12×10^{-12}	6×10^{-9}
II	4.24×10^{-11}	9.89×10^{-13}	1.61×10^{-12}	7.6×10^{-13}	3×10^{-9}
III	4.24×10^{-10}	9.89×10^{-12}	1.01×10^{-11}	7.6×10^{-12}	0
IV	2.12×10^{-8}	4.94×10^{-10}	5.05×10^{-10}	3.81×10^{-10}	0
V	1.64×10^{-7}	3.83×10^{-9}	3.94×10^{-9}	2.97×10^{-9}	0

Table 5. Power Series Expansion of Total Current Density in One Dimension

$$J_e = \frac{n e c}{2}\left(\frac{2kT}{\pi m c^2}\right)^{1/2} e^{-e\phi/kT} = J_{e_o} e^{-e\phi/kT}$$

$$J_i = \frac{1}{40} J_e e^{e\phi/kT} = J_{i_o} e^{e\phi/kT}$$

$$J_{e/_{eo}} = J_{e_o}(7.4)\frac{S_{max}}{E_{max}}\left\{1 - e^{kT/E_{max}}\left(\frac{\pi kT}{E_{max}}\right)^{1/2}\left[1 - \mathrm{erf}\left(\left(\frac{kT}{E_{max}}\right)^{1/2}\right)\right]\right\}$$

$$J_{ele} = J_{e/_{eo}} e^{+2e\phi/kT}$$

$$J = J_{hu} + J_i + J_{e/_e} - J_e$$

$$J = (J_{hu} + J_{i_o} + J_{e/_{eo}} - J_{eo}) + (J_{i_o} + 2J_{e/_{eo}} + J_{eo})\left(\frac{e\phi}{kT}\right)$$

$$+ (J_{i_o} + 4J_{e/_{eo}} - J_{eo})\,1/2\left(\frac{e\phi}{kT}\right)^2 + (J_{i_o} + 8J_{e/_{eo}} - J_{eo})\,1/6\left(\frac{e\phi}{kT}\right)^3$$

$$+ (J_{i_o} + 16J_{e/_{eo}} - J_{eo})\,1/24\left(\frac{e\phi}{kT}\right)^4 + \ldots$$

*One-half maximum values,

In addition to the thermal cdrreht,. the spacecraft Will see a current due to the relative veldcity of the spacecraft and the plasma. This Is called a ram current, Typical ram currents are shown in Table 6. Both the electron and ion currents will be increased by the ram current on surfaces facing into the velocity vector. Both currents will be reduced ob surfaces hidden from the velocity vector. Table 7 compares ram and thermal currents for the Pioneer Venus Orbiter. In Region I, the relative velocity is that of the solar wind. In Regions II through V, the relative velocity is the velocity of the spacecraft in its orbit. In Regions I and II, the photocurrent dominate8 and ram currents will have little effect on the net spacecraft charge. In Regions III, IV and V, the ram current will tend to make the Spacecraft potentials more positive.

Table 6. Ram Currents

Region, km	<V>, km/sec	per an3	J, A/cm^2
>1000	600.00	10	8×10^{-11}
1000	9.16	100	1.5×10^{-11}
700	9.38	1000	15×10^{-10}
350	9.66	5×10^{4}	7.7×10^{-9}
200	9.78	5×10^{5}	7.6×10^{-8}

Table 7. Likely Effect of Ram Currents

Region, km	Thermal J_{rain}	Thermal $J_{e_{max}}$	Thermal $J_{i_{max}}$	Comment
>1000	$e \times 10^{-11}$	3×10^{-10}	10^{-12} $6 \times$	Photocurrent dominates; ram current will make no difference to charge state of spacecraft; may influence experiments.
1000	16×10^{-11}	8×10^{-11}	2×10^{-12}	Greatly increases J_{i_e}; no effect when phase near zero; will tend to make spacecraft voltage mbre positive.
700	1.5×10^{-10}	8×10^{-10}	2×10^{-11}	
350	7.7×10^{-9}	4×10^{-8}	1×10^{-9}	
2w	7.8×10^{-8}	3×10^{-7}	$e \times 10^{-9}$	

3. SPACECRAFT ELECTRICAL MODEL

The electrical model for the brbiter includes more than 140 electrical elements and over 7d nodes, each representing an important spacecraft location (see Figure 2). This electrical model was constructed as described in7 and the following discussion outlines the formulation of the models.

3.1 Thrust Cone (Series 10)

The magnesium thrust cone was modeled as a series of linear indhctbrs arid resistors. A central node was used to provide a location for a capacitance to the surrbunding solar panel substrate. The lower end of the cone was tied directly to the equipment shelf support struts and the upper end represented the interface with the BAPTA and equipment shelf,

3.2 Equipment Shelf Support Struts (Series 20)

The 12 support struts were reduced to an equivalent configuration of four tb fit the simplified quadrant model of the equipment shelves and surrounding solar panels and substrate. The four strut elements were then modeled as linear inductors and resistors. Estimated resistances of bonded joints were included where it was felt important.

3.3 Equipment Shelf (Series 30)

The equipment shelf was modeled in quadrants with circumferential arid radial inductances and resistances calculated for each. A capacitance to the forward aluminum mesh and thermal blanket was alsb included. (Where two capacitances appear in series with an unimportant intervening node and one is much larger in magnitude than the other, the larger capacitance is omitted from the model for simplification, or an equivalent calculated.)

3.4 BAPTA and BAPTA Support Cone (Series 40)

The BAPTA and Its support strueture were modeled as an inductor and resistor tied at the ends to the equipment shelf and the main antenna supports.

3.5 Main Antenna Support, Dish, and Forward Omni (Series 50)

The aluminum antenna support structures were modeled as linear inductors and resistors with ti node at the main dish aiid at the omni. Capacitances were calculated for the: dish and the omnl to infinity. An esttmate of mutual inductance coupllng wlth the: antenna feed structure was also included.

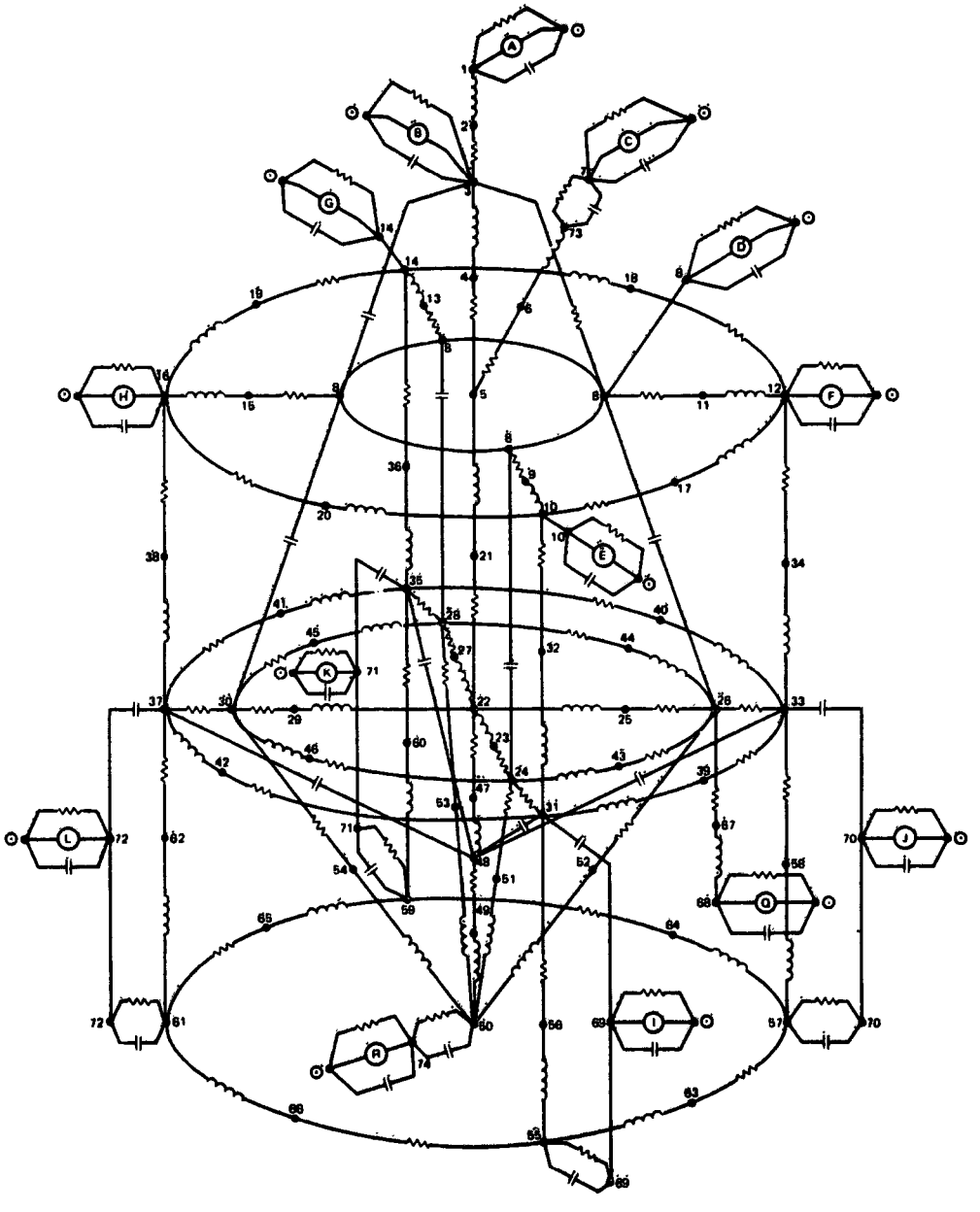

Figure 2. Pioneer Venus Electrical Model

KEY TO FIGURE 2

NODE	LOCATION	NODE	LOCATION
⊙ (ZERO)	∞ (GROUND)	31, 32, 33, 34	MESH/SUBSTRATE UPPER SECTION (LONGITUDINAL)
1	FORWARD OMNI (TOP OF MAST)	35, 36, 37, 38	AND SOLAR ARRAY INTERFACE
2	OMNI/ANTENNA SUPPORT	39, 40, 41, 42	SOLAR ARRAY TOP (CIRCUMFERENTIAL)
3	ANTENNA/SUPPORT MAST	43, 44, 45, 46	EQUIPMENT SHELF (CIRCUMFERENTIAL)
4	SUPPORT MAST	47, 48	THRUST CONE (UPPER)
5	MAST/BAPTA INTERFACE	49, 50	THRUST CONE (LOWER)
6	ANTENNA FEED SUPPORT	51, 52, 53, 54	EQUIPMENT SHELF SUPPORT STRUTS
7	ANTENNA FEED	55, 56, 57, 58	SOLAR ARRAY (LONGITUDINAL)
8	FORWARD [illegible]/THERMAL BLANKET	59, 60, 61, 62	
9, 11, 13, 15	FORWARD [illegible]/THERMAL BLANKET	63, 64, 65, 66	SOLAR ARRAY BOTTOM (CIRCUMFERENTIAL)
10, 12, 14, 16	MESH/SUBSTRATE UPPER SECTION (RADIAL)	67	AFT OMNI SUPPORT
17, 18, 19, 20	MESH/SUBSTRATE UPPER SECTION (CIRCUMFERENTIAL)	68	AFT OMNI
21	BAPTA	69, 70, 71, 72	SOLAR ARRAY COVERGLASS
22	BAPTA/EQUIPMENT SHELF/THRUST CONE INTERFACE	73	ANTENNA FEED TOP
23, 24, 25, 26	EQUIPMENT SHELF (RADIAL)	74	AFT FACING SIDE
27, 28, 29, 30			

3.6 Antenna Feed Strut and Cap (Series 60)

The antenna feed structures were modeled as an inductor and resistor with a node at the feed. The capacitances to the feed cap and to infinity were included.

3.7 Solar Array and Substrate (Series 70)

The solar panel enclosure was modeled as an oblate spheroid in order to calculate a representative capacitance to infinity. It was then divided into quadrants and longitudinal and circumferential inductances calculated frbm the formulas for a lossless transmission line. Associated resistances were also apportioned. Capacitances were calculated between impbrtant elements within the solar array and to the thrust cohe.

3.8 Substrate Extension and Mesh Wrap (Series 80)

Capacitances and inductances were calculated in the same manner as those for the solar array. Resistances were apportioned ambng the quadrant members.

3.9 Forward Mesh and Thermal Blanket (Series 90)

Radial inductances and resistances were calculated for the quadrants of the forward barrier in the same manner as for the equipment shelf. The capacitance of the antenna dish to the equipment shelf is also included.

3.10 Aft Structure and Aft Omni (Series 100)

The aft omni support add omni antenna Were modeled similar to the forward omni.

4. ISPICE CALCULATION RESULTS

The results of the Table 3 currents used on the electrical model are presented in Table 8. In Regions I and II, the photocurrent was modeled as an offset sine functibn with the phase angle depending on the quadrant. For example, Source I has a phase of 0°, J Has a phase of 90°, etc. The offset is chosen to make the photocurrent maximum at 90° and zero at 270°. This overestimates the photocurrent per spin cycle. A rectified sine curve would better approximate the photocurrent. In these regions, the effect of this pulsating current is seen as an at: voltage on the perimeter of the shelf. The magnitude of this voltage is shown in Regions I arid II at the four shelf locations and for the exterior of the solar panel. The frequehcy for this oscillation is the reciprocal of the spacecrak spin period.

The bnly voltage to exceed 1 volt in Table 8 is that of the solar panel in Region II. Here we assume a fairly High photbcurrent and a very law plasma temperature and density. The electron current is predominately a thermal current, the only current available to neutralize the phbtocurrent. Therefore, positive potentials are possible.

Table 8. ISPICE Calculations – 85 Percent Porosity

	Altitude (max)	200	350	700	1000	>1000 km
	Region	V	IV	III	II	I
Node	ISPICE Run	PV6	PV5	PV4	PV3	PV2
1	Omni antenna	-3.4	-11	-37	<1	24
3	Dish antenna	-1.9	-9.8	.37	<1	24
7	Antenna feed	-1.6	-9.5	-42	<1	21
8	Mesh	-1.9	-9.2	-37	<1	24
16	Solar panel extension	-1.8	-9.2	-37	<1	24 ± 0.04
22	Center of shelf	-1.8	9.2	-37	<1	24
24	Shelf 0°	-1.9	-9.2	-37	<1 ±4 μ	24 ± 0.04μ
26	Shelf 90°	-1.9	-9.2	-37	<1	24
20	Shelf 180°	-1.9	-9.2	-37	<1	24
30	Shelf 270°	-1.9	-9.2	-37	<1	24
72	Solar panel	-1.9	-0.2	-41	2344*	21 ± 20
74	Aft cavity	-37	-78	-91	-92	-54
R40N1	Current through BAPTA, μA	-2.3	-17	-1.1	13.6	-7.8

*±2333 mV.
NOTE: All voltages in millivolts unless otherwise noted.

Doubling the current densities in Table 2 will at most dobble the negative voltages for each region. In Regions I and II, the photocurrent dill dominates and the voltages remain about the same.

Increasing the conductive mesh area does not significantly change the potentials on the spabecraft. Table 9 shows a series of calculations in which the area of the conducttve mesh is calculated, assuming 0 percent porosity instead of 85 percent porosity. Modeling of the plasma and the spabecraft in this way is a new art and there are many areas of uncertainty. In extending thest! calculations, the ISPICE[8] representatioh of nonlinear voltage controlled current sources for low temperature plasmhs needs improvement, as does the representation of photocurrents on a spinning body. The effect bf ram currents as a function or Orbit position arid orientation, arid the investigation of sheath formatkn, plasma resistivity, and geometrical effects are also of interest.

Table 9. ISPICE Calculations – 0 Fercent Porosity

	Altitude (max)	200	350	700	1000	>1000 km
	Region	V	IV	III	II	I
Node	ISPICE Run	PV6	Pv5	PV4	PV3	PV2
1	Omni antenna	-3.4	-1 i	-40	<1	11
3	Dish antenna	-1.9	-9.8	-40	<1	11
7	Antenna feed	-1.9	-9.5	-42	<1	21
8	Mesh	-1.0	-9.2	-40	<1	10
16	Solar panel extension	-1.9	-9.2	-40	<1	10
22	Center of shelf	-1.9	-9.2	-40	<1	10
24	Shelf edge 0°	-1.9	-9.2	-40	<1	
26	Shelf edge 90°	-1.9	-9.2	-40	<1 ±4μ	10 ±13μ
28	Shelf edge 180°	-1.9	-9.2	-40	<1	10
30	Shelf edge 270°	-1.9	-9.2	-40	<1	10
72	Solar panel	-1.9	-9.3	-40	2344'	21
74	Aft cavity	-37	-78	-91	-92	-54
R40N1	Current through BAPTA, μA	-2.4	-18	-0.5	13.6	33

'±2333 mV.
NOTE: All voltages in millivolts unless otherwise noted.

References

1. Cloutier, P.A., et al (1974) Planetary Space Science, 22:967-990.
2. Kumar, S., and Hunten, D. (1974) J. Geophys. Res. 79(No. 16):2529-2532.
3. Stewart, R.W. (1971) J. Atmos. Sci. 28:1069-10...
4. Whitten, R.C., and Colin, L. (1974) Rev. of Geophys. and Space Physics 12(No. 2):155-192.
5. Binder, D., Smith, E.C., and Holman, A.B. (1975) IEEE Transactions on Nuclear Science NS-222(No. 6):2675-2680.
6. Spitzer, L. Jr. (1962) Physics of Fully Ionized Gases, Interscience.
7. DEMP Analysis of HS-3XX Spacecraft (1974) Intelcom Rad Tech, INTEL-RT 6045-004.
8. ISPICE Reference Guide (1974) National CSS, Inc., (Proprietary to NCSS, Inc).